PCCP

Accepted Manuscript

ROYAL SOCIETY OF CHEMISTRY

www.rsc.org/pccp

Cite this: DOI: 10.1039/c0xx00000x

www.rsc.org/pccp

FULL PAPER

Image molecular dipoles in Surface Enhanced Raman Scattering

Cristian Mihail Teodorescu*[a]

Received (in XXX, XXX) Xth XXXXXXXXX 20XX, Accepted Xth XXXXXXXXX 20XX
DOI: 10.1039/b000000x

The Surface Enhanced Raman Scattering (SERS) effect is explained using the interaction of a polarized molecule with its instantaneous image dipole in a metal surface. This model explains why SERS is obtained mostly on noble metals (Au, Ag), since these metals have usually lower inherent contamination as compared with other, more reactive, metals; thus, molecules may be found closer to the metal surface. It is shown how stronger SERS amplifications may be obtained using nanostructured surfaces, once the excited molecules are localized in concave sites. The dependence on the fourth power of the incoming radiation electric field is obtained by taking into account the dynamics of adsorption/desorption processes of molecules. The SERS effect is maximal when the excitation frequency is red-shifted with respect to the bulk plasmon resonance. Also, the SERS amplification factor may be dictated by the polarizability of the investigated molecule α in a much more critical way than just a power law α^2 or even α^4. By comparing the dipole induced charge density with the amplitudes of plasma waves, the domain of validity of the present theory is derived to be in the low separation regime, where the distance between molecules and metal substrates are below a few nanometres. Some data from the literature are analyzed in the framework of this model, namely the distance, frequency and temperature dependence of the SERS signal, all confirming the validity of the model.

Introduction

Although discovered almost four decades ago[1], the Surface Enhanced Raman Scattering (SERS) did not get so far a fully satisfactory explanation[2]. The initial proposed explanations were the 'chemical enhancement' (CE)[3] and the 'electromagnetic enhancement' (EME)[4]. As years passed, the latter was much more successful. At the same time, SERS data of increasing quality were available, achieving nowadays the ability to detect single molecules by this technique[5,6]. Since the basic electromagnetic mechanism proposed to explain the SERS effect stems in the use of 'surface plasmons' i.e. charge density waves in the metal oscillating in phase with the incoming radiation field, a whole domain named 'plasmonics' emerged during the last decade[7].

The key phenomenon in the EME theory may be summarized in three steps: (1) the incoming electromagnetic field generates a plasmon in the material, most often a surface plasmon (SP); (2) the field generated by this plasmon polarizes the molecule, in addition to the incident field (if one neglects retardation effects, i.e. if the involved molecule-substrate distances are well below the wavelength of the light); (3) the molecule emits Raman-shifted radiation. Therefore, in order to achieve high SERS amplifications, firstly a matching is sought between the frequency of the incident light and the SP frequency. Also, it was evidenced that surface nanostructuring yields to even enhanced SERS amplification factors[1,8-11]. This yielded to the fabrication of specially adapted SERS substrates[11,12], aiming to match the metal surface nanostructuring with either the light wavelength or with the SP wavelength. However, a disordered nanostructured gold-capped porous silicon substrate yielded a similar (even better) SERS amplification factor as the commercial SERS nanofabricated substrates[11]. Such observations yielded recently to the proposal of 'hotspots', mainly located in the concavities of metal surfaces or at the interface between metal nanoparticles[13,14]. Other actual researches based on the previous three step model of the SERS effect are the fabrication of nanoantennas[14,15] and studies of the light scattered by these nanostructures. The full theory of plasma excitation is rather complicated[7] and difficult to be directly used in order to quantify the SERS effect. The normal way to proceed in simulation is based on discrete methods, either finite difference time domain (FDTD)[12,14], two dimensional boundary element methods (2DBEM)[15] or discrete dipole approximations (DDA)[13,16]. The latter method already contains the ingredients of the method we will discuss in the following: but in the following we will propose that a single dipole is induced in the metal, which may be regarded as the image of the dipole induced in the investigated molecule, placed in the neighborhood of the metal surface.

For arrays of ordered metal nanoparticles, a clear SERS enhancement is observed when the polarization of the exciting light is parallel to the rows of nanoparticles[17,18]. It was computed that the incident intensity (proportional to the square of the electric field E^2) may be enhanced by a factor of several thousands for spheres of about 20 nm diameters separated by a gap of 1 nm, right in the middle of the gap[17]. Therefore, since the SERS enhancement factor may be parametrized as depending on E^4 (see below), enhancement factors of ~ 10^6-10^7 are to be expected to be produced by such 'hotspots'.

The key quantity which will be computed in the actual paper is the molecular polarizability α, which is the proportionality constant between the applied electric field and the dipole moment induced in a molecule $\boldsymbol{P} = \alpha \boldsymbol{E}$. (Throughout this work we will neglect any eventual tensor character of the polarizability.) Indeed, the Kramers-Heisenberg formula[19] shows that the intensity of the Raman scattering is proportional to $\alpha^2 E^2$, the proportionality with E^2 originating from the intensity of the exciting field.

A brief review of orders of magnitude implied in SERS follow. The incoming electric field of a light source with flux of ~ 10^4 W/m^2, providing ~ 2 x 10^{22} photons/(m^{2}s) with individual energy of 3 eV, is of about 3 x 10^3 V/m. The molecular polarizability may be written as $\alpha = 4\pi\epsilon_0 V_p$, where V_p is the 'polarization volume of the molecule', on the order of 1-1000 Å^3 (Ref. [20]), and ϵ_0 is the permittivity of the vacuum. Therefore, the molecular polarizability is on the order of 10^{-37}-10^{-40} Fm^2, and in the above electric field a molecule will develop an instantaneous dipole moment of about 10^{-4}-10^{-7} D (1 D ≈ 3.34 x 10^{-30} C·m ≈ 0.2 e·Å).

The main features of SERS are: (i) the enhancement factor is from 10^4 to 10^{10} or even higher[1,5,6]; (ii) the predominance of SERS when using noble metal surfaces (Au, Ag); (iii) the further enhancement of SERS due to nanostructured substrates; (iv) the dependence of SERS on the fourth power of the electric field E^4; (v) the strong dependence on the distance d between the molecule and the substrate reported so far ~ $(d + \text{const.})^{-10}$, according to Refs. [9,10]; (vi) the SERS enhancement when the exciting frequency approaches the plasmon frequency of the metal[1,9,10].

In this paper we will present a simpler model, based on the interaction of an instantaneously polarized molecule with its image dipole formed by the metal surface. This phenomenon is supposed to occur instantaneously, as opposed to the three-step model described a few paragraphs above (see the 'AOA' mechanism proposed in Ref. [14] for the surface-enhanced light scattering). Without discarding the presence of plasmons, it will be shown that the actual model, based on simple considerations on electrostatics, mechanics, and thermodynamics, accounts for the origin of the SERS effect and for all features (i-vi) described above. From the very beginning, we must emphasize that the basic aspects of the theory presented in the following are valid especially when the separation distances from molecules to substrates are in (or below) the nanometer range. These are the conditions for the field produced by the image dipole to be robust at the position of the molecule. Then, the effects of the surface nanostructuring will be investigated, and the main result will be that nanocavities with typical shapes in the nanometer range must be present by the substrate, in order to give a further enhancement. The next Subsection presents the effects of dynamic adsorption/desorption statistics and here also one needs to consider quite low distances in order to obtain an effective agglomeration of the molecules towards the surface, yielding a proportionality with the fourth power of the product between the exciting electric field and the polarizability. The next Subsection treats the dynamic case and ends with a comparison between the amplitudes of the charge modulations induced in the metal by the oscillating dipole, compared with the plasma oscillations. Here it will be demonstrated that in the nanometer regime of molecule-substrate distances the former contribution exceeds the later one. The final Subsection analyzes two practical cases, showing (i) how one can apply the model and derive the distance from analyzed molecules to the substrate when one knows the spectral dependence of the amplification factor and (ii) hw one can analyze the temperature dependence of the SERS amplification factor and how one can extract from these data the enhancement factor. The last Section, Discussions and Conclusion, summarizes the findings from this basic considerations and presents a survey of experiments to be achieved in the future to get more insight on the validity of the present work.

Results

Image dipoles

Classical electrostatics proposes that any charge near a metal surface whose potential is kept constant will induce a polarization of the free electrons in the metal which may be assessed outside the metal by introducing a virtual 'image charge'[21]. Therefore, dipoles must induce image dipoles. Such a situation is represented in Fig. 1. It is easy to estimate that the induced electric field at the original molecule by its image is $P/[4\pi\epsilon_0(2d)^3]$. Let α_0 be the polarizability of the molecule in absence of the metallic wall. Therefore, the total dipole moment given by the incident E_0 and the induced $E_{\text{ind.}}$ electric fields is given by:

$$P = \alpha_0\left(E_0 + E_{\text{ind.}}\right) = \alpha_0 E_0 + \frac{\alpha_0 P}{4\pi\epsilon_0 (2d)^3} \qquad (1)$$

From here, the 'effective' polarizability near the metal surface is computed simply as $P = \alpha E_0$, with:

$$\alpha = \frac{\alpha_0}{1 - \dfrac{\alpha_0}{4\pi\epsilon_0 (2d)^3}} = \frac{4\pi\epsilon_0 V_p}{1 - \dfrac{V_p}{(2d)^3}} \qquad (2)$$

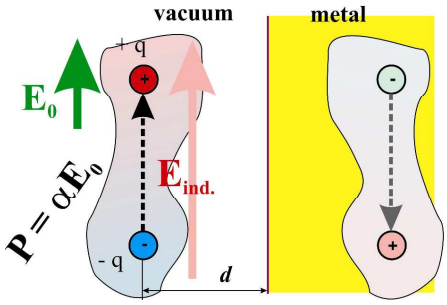

Fig. 1. Image dipole created into a metal surface. E_0 is the external field, $E_{\text{ind.}}$ is the induced field by the image dipole at the location of the original dipole.

These considerations are quite similar to the well known 'polarization catastrophe' in dielectrics, yielding eventually to ferroelectric ordering, with occurrence of permanent dipolar moments in absence of an applied field[22]. An important class of ferroelectrics (perovskites ABO_3) are formed by combining low ionic radius A cations (e.g. Ti^{4+}) with large ionic radius (and heavier) cations in lower charge states (e.g. Pb^{2+}), with a clear covalent character of the B-O bonds[23]. The BO planes could be viewed as monolayer sheets of metallic character, which may

image dipole moments produced by rumplings of the AO_2 atomic layers, yielding ferroelectricity in a quite similar mechanism as that described by eq. (2).

When the denominator of eq. (2) is small, i.e. when $2d \approx V_p^{1/3}$, the polarizability may increase dramatically. By taking into account the order of magnitude of the polarization volumes in absence of the metal surface (10-1000 Å^3), this implies distances from the molecule to the substrate ranging from 1 to 5 Å. Therefore, the proximity of the metal surface is *essential* for an increase in the molecular polarizability through this mechanism. That also implied that any non-conductive layer (such as the inherent contamination of most metals, which may be of several nm thickness[24]) will significantly reduce the SERS amplification factor by imposing a larger separation distance d between the molecule and the metal able to produce image dipoles. This might be the reason why SERS is mostly observed on noble metal surfaces, since the reactivity of these surfaces with the ambient atmosphere is minimal. Indeed, any highly surface sensitive technique, such as X-ray photoelectron spectroscopy, reveals that the contamination layers exceed about three times the photoelectron escape depth (1-1.5 nm) for most metals, except for Au, Ag and Pt, where the inherent contamination layer is less than ~ 1.5-2 Å thick (in the range of one single atomic layer)[25]. This is the case of metals in air and at atmospheric pressure; it is also true that the nature and the thickness of the contamination layer into a liquid (a solution, an electrolyte) may change dramatically.

When the excited molecule is located at equal distance between two metal walls, the induced field is almost twice the value from eq. (1), i.e. $E_{ind.} \approx 1.803\ P/[4\pi\epsilon_0(2d)^3]$. The factor of increase is not exactly two, owing to multiple imaging yielding a series $\Sigma_{k\geq 1}\ (-1)^{k-1}/k^3 \approx 0.901543$ in the overall field induced. However, this effect may explain the huge success of the tip enhanced Raman scattering (TERS) method[26].

A final remark on the above basic consideration is that the SERS amplification factor, as described by the square of the molecular 'effective; polarizability, eq. (2), depends on the molecule investigated and not only on the distance to the metal substrate. Actually, several factors may be foreseen to influence the SERS signal: (i) the nature of the molecule and its polarizability, via V_p; note that the dependence is not just a power law one (e.g. $\sim \alpha^n \sim V_p^n$), but rather involves approaching a divergence (ii) the contamination of the metal substrate or any other process yielding layers which separate the molecules from the substrate, via d; (iii) in absence of such contamination layer, the adsorption geometry of the molecule itself on the metal surface, supposing hat the molecule does not dissociate. In this last case, the 'chemical enhancement' mechanism has also to be taken into account.

In the following sections we will treat the other factors intervening in the SERS effect: the surface nanostructuring, statistical effects and the dependence on the excitation frequency.

Surface nanostructuring

Another feature of the SERS effect is the strong enhancement induced by surface nanostructuring[1,8,10-13]. The basic explanation of this effect is that plasmons are coupled to the geometry of the surface, therefore the plasma oscillation might be enhanced by a regular nanostructuring. In the following we will demonstrate that the actual model accounts for this effect in a quite natural way.

Suppose that a part of a nanostructured surface is formed locally by spherical caps, such as represented in Fig. 2. One may compute the force exerted between a dipole $P = q \times \delta_0$ and its image formed in such a spherical cap as:

$$F_a(d,0) = \frac{q^2}{8\pi\epsilon_0 d^2}\left[1 - \frac{1}{\left\{1+[\delta_0/(2d)]^2\right\}^{3/2}}\right] \approx \frac{3P^2}{4\pi\epsilon_0 (2d)^4}$$

for $\delta_0 << d$ (3)

A molecule of mass 100 Daltons carrying a dipole momentum of 10^{-5} D located 5 Å away from the surface will suffer an attraction acceleration of about 18 g towards the metal surface. Therefore, a mechanism such as that represented in Fig. 2 may be proposed for migration of molecules towards the concavities. Molecules subject to the interaction with two image dipoles will tend to migrate towards an equilibrium position in a concavity. For a distance of 50 nm to the surface the acceleration is lower (~ 1.8 x 10^{-6} m/s^2), but still important at the nanoscale level; the complete migration of a molecule over 100 nm takes place in less than one second, so within the time scale of the measurement.

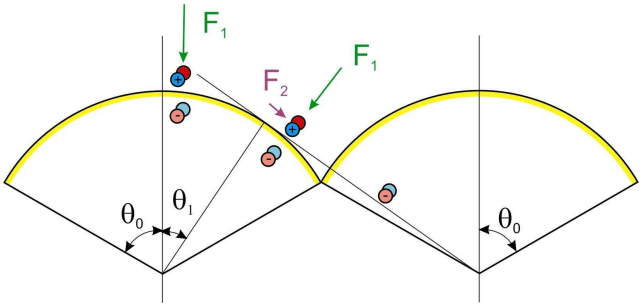

Fig. 2. Mechanisms of localization of target molecules inside concavities

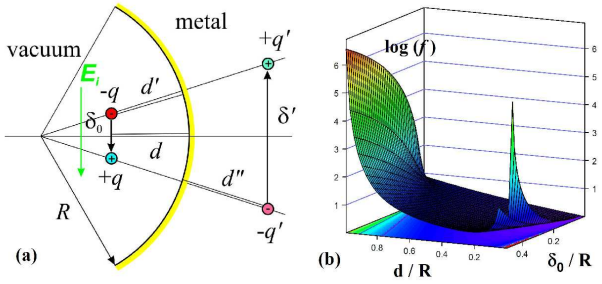

Fig. 3. (a) Image dipole produced by a concave metal surface. (b) Enhancement factor f due to the presence of concavities (note the $\log_{10}$ scale).

The next step is to evaluate the induced field by an image dipole created by a concave metal surface (Fig. 3a). The induced field will be enhanced by a factor which will be called 'nanostructuring factor' f, defined as the ratio between the induced field in the case of a concave metal surface and the induced field by a plane metal surface:

$$\frac{E_i}{E_i^{(0)}} = \frac{\left(\frac{2d}{R}\right)^3\left[\left(1-\frac{d}{R}\right)^2+\left(\frac{\delta_0}{2R}\right)^2\right]^2}{\left(1-\frac{d}{R}\right)^4\left[\frac{2d}{R}-\left(\frac{d}{R}\right)^2-\left(\frac{\delta_0}{2R}\right)^2\right]^3} \equiv f\left(\frac{d}{R},\frac{\delta_0}{R}\right) \approx \left(\frac{2R}{2R-d}\right)^3 \quad \text{for } \delta_0 << d, R \quad (4)$$

The values obtained for this factor could go until several orders of magnitude when $d \rightarrow R$ and $\delta_0 \rightarrow R/2$. In practice, when R is in the nanometre range, and by using typical distances between the molecule and the surface of some 5 Å, several units are derived for the shape enhancement factor f.

The complete function in eq. (4) becomes infinite when $d \approx R$, i.e. when the molecule is placed in a centre of a hemispherical cavity or of a spherical surface exceeding one half sphere. This could correspond to the situation where the metal (at least) half sphere is filled with a fluid containing the analyzed molecules; thus, the strongest image dipole induced field acts on molecules from the centre of this sphere. A more realistic real situation implies that the analyzed molecules may be found near the centre of the hemisphere within some uncertainty Δd: $d \approx R \pm \Delta d$ /2, where $\Delta d << R$. Introducing this in eq. (4) one finds, with a good approximation that the enhancement factor $f \approx 8\,[1 + (\delta_0/\Delta d)^2]^2$. If the molecules could be fixed near the centre of the hemisphere within a better precision than the charge separation in the dipole, the geometric enhancement factor may become considerable. For example, if $\delta_0/\Delta d \approx 10$, then $f \approx 8 \times 10^4$. This stabilization should occur in a time scale on the order of the inverse of the light frequency (ν^{-1}), in the range of 10^{-15} s for optical photons. The position fluctuation during one cycle of light may be written as $\Delta d \approx \langle v \rangle / \nu$, where $\langle v \rangle$ is the average thermal speed of these molecules: $(3k_BT/m)^{1/2}$ ~ several hundreds of m/s in gases, where m is the molecular mass and k_BT the Boltzmann factor. In liquids or solids, the average thermal speed may be lower. It follows that Δd is on the order of 0.001-0.01 Å. Next, the evaluation of δ_0 is rather difficult (*ab initio* computations of the molecular electronic structure in an applied film are needed); from the optical properties (dipole moment) all we know is its product with the charge q. However, one could make the ansatz that δ_0 is at least on the order of a bond length, a few Ångströms. Thus, the estimated geometric enhancement factor in the centre of a hemisphere might be even larger than the value estimated above. It may happen that when a fluid is accumulated inside a nanometre sized hemispherical cavity, most of the signal is provided by molecules placed in the centre of this cavity. Thus, one may foresee a quite simple explanation for 'hotspots'.

The formula for the polarizability modified by the nanostructured surface must be modified by including the nanostructuring factor f, as follows:

$$\alpha = \frac{\alpha_0}{1-\frac{\alpha_0 f(d/R,\delta_0/R)}{4\pi \in_0 (2d)^3}} = \frac{4\pi \in_0 V_p}{1-\frac{V_p f(d/R,\delta_0/R)}{(2d)^3}} \quad (5)$$

Therefore, easier conditions are obtained for lowering the denominator of eq. (5) if this factor is present. An abbreviation such as CERS (= Cavity Enhanced Raman Scattering) may be introduced to account for this phenomenon [17]. Also, the presence of a convex surface (such as a tip) *alone, without an associated metal counter-electrode* will yield to a *decreasing* factor f. Note also that, in any case, no regular array of concavities is needed to explain the enhancement. The real surface nanostructuring with concavities as small as possible (though not smaller than the typical dimensions of the molecule) is enough to provide a robust enhancement, as evidenced in Ref. [11]. Gold substrates with ~ 1 nm nanogaps provided recently SERS enhancement factors in the range of 10^8 - 10^9, see e.g. Ref. [27].

When the denominator of eq. (5) becomes negative, the molecule, which initially was assumed to not carry a permanent dipole moment, will become polarized or even dissociated near the metal surface. The mechanism is the following: first of all, even in absence of exciting radiation, molecules are undergoing instantaneous polarizations owing to their interaction with thermal radiation or to vacuum fluctuations of the electromagnetic field. As soon as a molecule approaches a metal surface, its eventual instantaneous polarization will be amplified by the effect described previously. When the amplification factor $\{1 - V_p f/(2d)^3\}^{-1}$ is strong enough, there are two possibilities: (i) the molecule is broken; (ii) the molecule stabilizes in a polarized state. For understanding these two phenomena, one should consider the nonlinearity of the polarization dependence $P_0(E)$ for the isolated molecule. Considering the next term in a series development of the polarization *vs* field $P_0(E) \approx \alpha E + \beta E^2$, when the parameter $\beta > 0$, any increase of the applied field (including the field due to the image dipole) yields a more dramatic increase of the dipole moment, up to the dissociation of the molecule. When $\beta < 0$, one can imagine that the polarization saturates as function on the applied field. Therefore, the molecule is stabilized in the polarized state, which does not increase anymore. Other interesting predictions are the natural induction of ferroelectricity in an ensemble of adsorbed molecules on a metallic substrate; these findings will be detailed in a subsequent work, which will include also the analysis of polar molecules (molecules carrying a dipole moment in absence of any interaction). Anyway, some spectroscopic evidences could be sought about the fact that molecules subject to SERS measurements are initially polarized. Actually, there are quite often spectral differences between SERS and conventional Raman spectra of the same molecule; this is usually attributed to charge transfers or other chemical effects[28]. As mentioned above, in he physics of ferroelectrics, the 'polarization catastrophe' is derived from a similar formalism and it yields to the stabilization of a spontaneous electric polarization inside the material[22,29].

Dynamic adsorption/desorption: E^4 enhancement and dependence on distance to the metal substrate

Once the adhesion force is computed by eq. (3), it is easy to estimate the adhesion energy, i.e. the work necessary to detach the molecule which is found initially at a distance z from the substrate:

$$U_a(z) = -\int_z^\infty F_a(z')dz' \approx -\frac{P^2}{8\pi \in_0 (2z)^3} \equiv -\varepsilon_0(z) \quad (6)$$

By using convenient units $|\varepsilon_0|$(meV) ≈ 39 P^2(D)/z^3(Å). As a consequence, even at sub-nanometre distances from the surface, molecules will have adhesion energies on the order or lower than the thermal energy (about 25 meV at room temperature). Now suppose that the target molecules are in a gas or in a liquid, obeying Botzmann statistics. The density increase near the surface (z = 0) may be expressed as:

$$\Delta n(z) = n_0\left[\exp\left(\frac{\varepsilon_0(z)}{k_B T}\right)-1\right] \approx n_0 \frac{P^2(z)}{8\pi \in_0 (2z)^3 k_B T} \qquad (7)$$
$$= \frac{n_0}{8\pi \in_0 (2z)^3 k_B T}\alpha^2(z)E^2$$

n_0 being the initial density, $\alpha(z)$ the z-dependent polarizability and E the exciting electric field. The last function from eq. (7) is a rapidly decreasing function on z. We consider that the minimal distance from the molecule to the substrate $d_{min.}$ is close to (but larger than) the singularity of $\alpha(z)$, i.e. $2d_{min.} = (V_p f)^{1/3} + b$, b being a small quantity. The overall SERS enhancement provided by molecules at a distance z in a layer dz may be written as:

$$dI_{SERS} \propto E^2\alpha^2(z)\Delta n(z)dz\Delta S \propto \frac{E^4\alpha^4(z)}{(2z)^3 T}dz\Delta S \qquad (8)$$
$$\propto \frac{{\alpha_0}^4 E^4}{T}\cdot\frac{(2z)^9}{\left[(2z)^3 - V_p f\right]^4}dz\Delta S$$

ΔS being the area investigated. To compute the overall enhancement, one must integrate the above z dependence from $z = d_{min.}$ to infinity. The integral can be computed analytically and it follows that the dependence on the spatial distance to the metal substrate is on the form:

$$I_{SERS} \propto \frac{201\xi}{\xi^3-1}+\frac{171\xi}{(\xi^3-1)^2}+\frac{54\xi}{(\xi^3-1)^3}-14\log\frac{(\xi-1)^2}{\xi^2+\xi+1} \qquad (9)$$
$$+28\sqrt{3}\left\{\tan^{-1}\left(\frac{1+2\xi}{\sqrt{3}}\right)+\frac{\pi}{2}\right\}$$

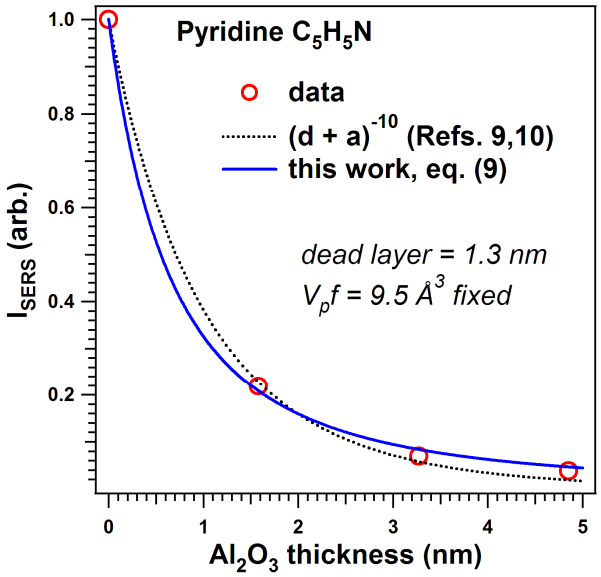

Fig. 4. Fits of the dependence of the SERS signal on the Al_2O_3 spacer to Ag films grown on nanospheres (AgFON). The data are extracted from Refs. [9,10].

where $\xi = 2d_{min.}/(V_p f)^{1/3}$. This implies a quite strong dependence on the separation distance between the molecules and the substrate. This is not exactly the $(d + a)^{-10}$ law proposed in Refs. [9,10], but its behavior is quite close, i.e. it is a function strongly decreasing with d. The data from Refs. [9,10] may be fitted quite well with formula (9), as shown in Fig. 4. An additional fitting parameter regarded as a 'dead layer' (d_0) was introduced additionally to improve the quality of the fit, such that in this case $t = 2(d + d_0)/(V_p f)^{1/3}$. This 'dead layer' of about 1.3 nm thickness may be seen as an inherent contamination of the Ag film or some other effects preventing pyridine molecules to agglomerate exactly on the Al_2O_3 spacer. The molecular polarizability was fixed, V_p = 9.5 Å^3 for pyridine[20]. The fit with the $(d + a)^{-10}$ law is also represented. The fit by using eq. (9) is slightly better (and the number of fitting parameters is the same), the χ^2 of the fit is lower by about 40 %. To draw a definitive conclusion, we suggest that more such experimental data on SERS signals dependence on insulating spacers need to be investigated. Note also the $1/T$ dependence. This could be a sign that improved SERS signals may be obtained at low temperatures.

The proportionality of the SERS intensity with the fourth power of the polarizability and of the exciting electric field is a significant effect. A SERS enhancement factor of four orders of magnitude may occur if the polarizability increases by one order of magnitude only.

In fact, for dipole moments of ~ 1 D the adhesion energies may exceed the thermal energy, therefore in this case the development of the exponential in eq. (7) might not be appropriate. This should happen with molecules carrying permanent dipole moments (P_p). The overall dependence of SERS will be in this case as $E^2\alpha^2\{\exp[ct.(P_p + \alpha E)^2/T)-1]$, more abrupt than $(\alpha E)^4$. For dipole moments of ~ 10^{-4}-10^{-5} D, i.e. with no permanent dipole moments and low polarizability, the adhesion energy is quite low compared with the thermal energy and it might happen that no significant increase of the density near the surface occurs; in this case, the SERS intensity remains proportional to $(\alpha E)^2$. Consequently, the 'E^4 enhancement' might not be an universal law, according to the present considerations.

Some examples concerning the temperature dependence of the SERS signal will be discussed in a later paragraph.

Charge density analysis in the dynamic case: image dipoles vs. surface plasmons

We will firstly consider the charge density in the metal for the static case. One assumes that the charge distribution on the metal surface generates an electric field which compensates the in-plane electric field generated by the external charge. By applying the in-plane divergence on this induced electric field, one may compute the associated induced charge density on the surface. For a dipole $P = q\delta_0$ consisting in a charge (+ q) located at (x = - $\delta_0/2$, y = 0, z = - d) and a charge (- q) located at ($x = \delta_0/2$, y = 0, z = - d), the induced charge distribution on the surface (z = 0) is given by:

$$\rho_{ids}(x,y)=\frac{q}{4\pi}\times$$
$$\times\left\{\frac{\left(x+\frac{\delta_0}{2}\right)^2+y^2-2d^2}{\left[\left(x+\frac{\delta_0}{2}\right)^2+y^2+d^2\right]^{5/2}}-\frac{\left(x-\frac{\delta_0}{2}\right)^2+y^2-2d^2}{\left[\left(x-\frac{\delta_0}{2}\right)^2+y^2+d^2\right]^{5/2}}\right\} \quad (10)$$
$$\approx\frac{3Px\left(4d^2-x^2-y^2\right)}{4\pi\left(x^2+y^2+d^2\right)^{7/2}} \quad \text{for } \delta_0 << x,y$$

were the index *ids* stands for 'induced-dipole-static'. These dependencies are represented in Fig. 5, as functions on x/d and y/d, for δ_0/d = 0.02, which roughly correspond to an external dipole or 1 D ≈ 1 e x 0.2 Å and to a separation distance d = 1 nm. It may be seen that the approximation is quite reasonable, consequently this approximation will be used in the following. For lower values of the charge separation inside the dipole δ_0, the approximation is even better.

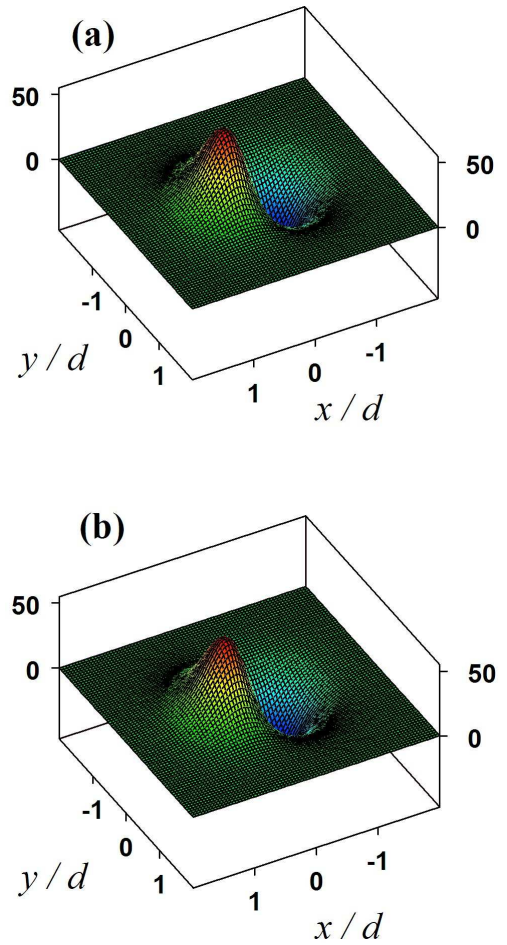

Fig. 5. Charge density distribution due to a dipole with δ_0/d = 0.02: (a) exact formula, second term from eq. (10); (b) 'approximate' formula in eq. (10). The units of charge density are $q/(32\pi d^3)$ x 10^{-3}.

The next step is to treat the dynamic case, i.e. to assume a periodic electric field excitation of frequency ω: $E_0\cos(\omega t) = E_0$ Re $\exp(i\omega t)$. All calculation will be performed by using complex numbers and the convention is to take the real part at the end. Within this formalism, the high frequency behaviour of the metal is described by the Drude-Zener conductivity[30]:

$$\sigma(\omega)=\frac{\sigma_0}{1+i\omega\tau_1} \quad (11)$$

where τ_1 is the relaxation time, $\tau_1 \approx <\tau(\varepsilon_F)>$, on the order of 10^{-14} s for most metals.

Apart for τ_1, another time interval will occur in the formulas below, it is given by the ratio between the vacuum permittivity and the static conductivity $\tau_0 = \epsilon_0/\sigma_0$; this is on the order of 10^{-18}-10^{-19} s for good conductors. It is easy to introduce the plasma frequency as the inverse of the geometric mean of these two times; $\omega_p = (\tau_0\,\tau_1)^{-1/2} = (ne^2/m^*\epsilon_0)^{1/2} \sim 10^{16}$ s^{-1}, where n is the electron density in the metal, and m^* their effective mass. Now, for real experiments, the excitation ω is close (though not exceeding) ω_p and therefore $\omega\tau_1 \sim \omega_p\,\tau_1 \sim 10^2 >> 1$ and $\omega\tau_0 \sim \omega_p\,\tau_0 \sim 10^{-2} << 1$.

The following step is to use at the same time the continuity equation and the first Maxwell equation, as follows:

$$\begin{aligned}&\operatorname{div}\boldsymbol{j}=\sigma(\omega)\operatorname{div}\left(\boldsymbol{E}_{ext}(\boldsymbol{r},t)+\boldsymbol{E}_{ind}(\boldsymbol{r},t)\right)\\&=-\sigma(\omega)\frac{\rho_{ids}(\boldsymbol{r})}{\epsilon_0}e^{i\omega t}+\sigma(\omega)\frac{\rho_{id}(\boldsymbol{r},t)}{\epsilon_0}=-\frac{\partial\rho_{id}}{\partial t}\end{aligned} \quad (12)$$

The first term is the external field produced by the dipole; its spatial dependence is given by eq. (10), where one simply replaces the static dipole moment P by the amplitude of the oscillating dipole P_0. Assuming now that the charge in metal oscillates with the same excitation angular frequency ω, replacing the Drude-Zener conductivity $\sigma(\omega)$, the charge induced in the metal is expressed as $\rho_{id}(\boldsymbol{r}, t) = \rho_0(\boldsymbol{r})\exp(i\omega t)$, where ρ_0 is complex, to account for eventual phase shifts. Replacing ρ_{id} in eq. (12), one obtains $\rho_0(\boldsymbol{r}) = \rho_{ids}(\boldsymbol{r})\,\{1 + i\omega\tau_0(1 + i\omega\tau_1)\}^{-1}$ and by taking the real part of $\rho_{id}(\boldsymbol{r}, t)$, this yields the time-dependent charge induced at the metal's surface:

$$\rho_{id}(\boldsymbol{r},t)=\rho_{ids}(\boldsymbol{r})\frac{\left(1-\frac{\omega^2}{\omega_p{}^2}\right)\cos\omega t+\omega\tau_0\sin\omega t}{\left(1-\frac{\omega^2}{\omega_p{}^2}\right)^2+\omega^2\tau_0{}^2}\approx$$
$$\approx\rho_{ids}(\boldsymbol{r})\frac{\left(1-\frac{\omega^2}{\omega_p{}^2}\right)\cos\omega t}{\left(1-\frac{\omega^2}{\omega_p{}^2}\right)^2+\omega^2\tau_0{}^2}\equiv-\rho_{ids}(\boldsymbol{r})g(\omega)\cos\omega t\approx\frac{\rho_{ids}(\boldsymbol{r})\cos\omega t}{1-\frac{\omega^2}{\omega_p{}^2}} \quad (13)$$

The molecular dipole oscillates as cos ωt. Therefore, to a good approximation, the charge in the metal oscillates in phase with the dipole. Here and in the following we will neglect retardation effects, since these effects will occur when the distance d between the dipole and the surface approaches the wavelength, which in actual experiments is of several hundreds of nm, whereas we consider d in the range of 1 nm. The intensity of the oscillations increases when the excitation frequency approaches

the plasmon frequency; however, it does not diverge when $\omega = \omega_p$, as the last approximation of eq. (13) suggests. The function $g(\omega)$ exhibits extrema when $\omega = \omega_p (1 \pm \omega_p \tau_0)^{1/2} \approx \omega_p \pm 1/(2\tau_1)$. In terms of wavenumbers, the extrema are shifted by approximately $1/(8\pi c \tau_1)$ with respect to the plasmon frequency.

The term with (sin ωt) becomes dominant when the excitation frequency approaches the plasma frequency. In this case, the charge in the metal oscillates with a phase shift of $\pi/2$ with respect to the excitation wave. However, this field, when transmitted back to the excited molecule which vibrates as (cos ωt), will produce no net effect from classical theory in terms of absorbed power from the radiation field, since the average of the product (sin ωt cos ωt) is zero.

In the Electronic Supplementary Information (ESI), the case of corrections due to penetrating field into the metal is analyzed. The charge density in the (z = 0) plane oscillating in phase with the dipole ($\sim P_0 \cos\omega t$) may be written in this case such as:

$$\tilde{\rho}(x,y,z=0,t) \approx \frac{3P_0 x \cos\omega t}{4\pi\left(x^2+y^2+d^2\right)^{7/2}\left\{\left(1-\frac{\omega^2}{\omega_p^{\,2}}\right)^2+\omega^2\tau_0^{\,2}\right\}} \times\left\{\left(1-\frac{\omega^2}{\omega_p^{\,2}}\right)\left[3\left(4d^2-x^2-y^2\right)-5\kappa_0 d\left(x^2+y^2+d^2\right)\right] -5\omega\tau_0\kappa_0 d\left(x^2+y^2+d^2\right)\right\} \quad (14)$$

where $\kappa_0 = [\omega/(2\tau_0)]^{1/2}/c$ is the inverse of the skin depth (see the ESI). It is easy to estimate that the correction term is important only when d becomes comparable with $\kappa_0^{-1} \sim$ 4-5 nm. In Fig. 6 the spatial dependence of the leading term of eq. (14) is represented for several values of the product ($\kappa_0 d$). This figure may be viewed as a 'thought experiment' of what happens when the distance between the molecule and the metal surface is increased. At the beginning, the amplitude of the surface charge density is quite similar to that represented described by eq. (10) and plotted in Fig. 5.

Starting with $\kappa_0 d \approx 1$, the charge density starts to exhibit 'ripples' which can also be described as surface plasmons. Interestingly, by about $\kappa_0 d \approx 2$ the shape of the surface density is reversed, in that the charge density starts to have the same sign as the ion sitting on the area in question (electrons accumulate on the side of the negative ion). Physically, this inversion happens at distances of about 10 nm. This could also correspond to a dynamic *repulsion* between the molecule and the surface. In the following, we will derive the critical distance where the surface charge density given by the direct excitation of plasmons with the incoming electromagnetic wave prevails with respect to the charge density generated by the oscillation of the molecular dipole. It will be seen that in this distance range (above 10 nm) the plasmon charge density dominates.

The evaluation of the charge induced by the electromagnetic wave into the metal (the plasmons) and the comparison of this charge modulation with the charge density induced by the dipole is based on the following main ideas:

(i) The electromagnetic wave hits the surface at an angle θ_0; the incidence plane is the (y = 0) plane.

(ii) The electromagnetic wave may present two polarizations: s and p, where p stands for polarization in the incidence plane and s for polarization normal (senkrecht) to this plane. It may be easily demonstrated that only the p wave is able to excite surface plasmons.

(iii) The electromagnetic wave is totally reflected by the metal and the reflected wave acquires a phase shift of π with respect to the incident wave.

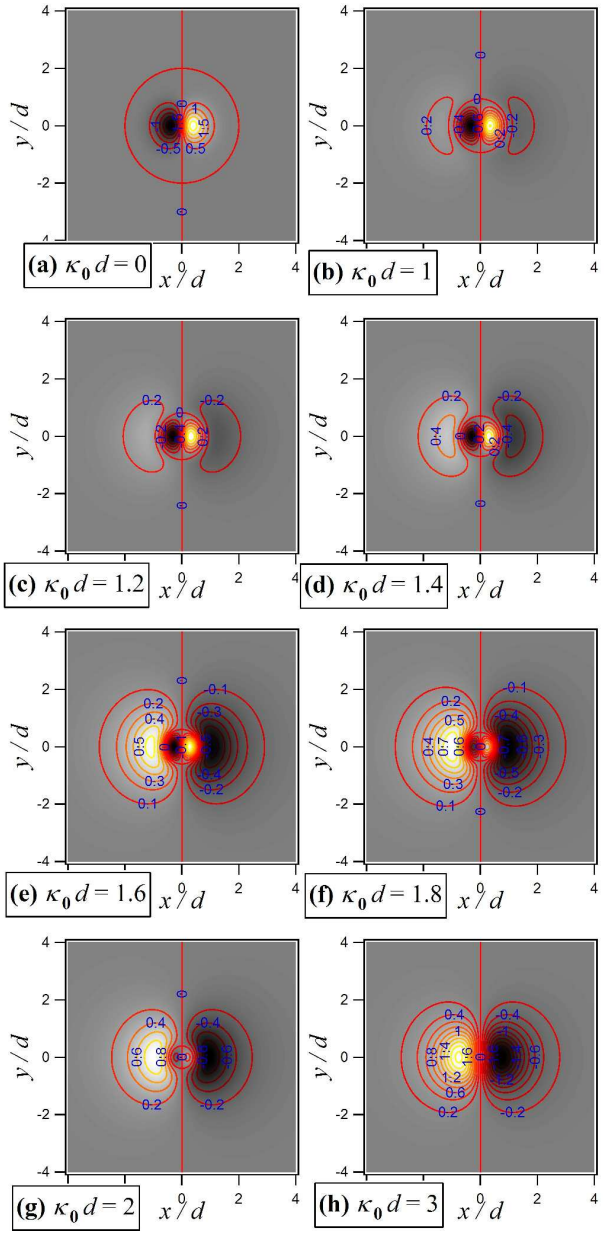

Fig. 6. Evolution of the amplitude of the surface charge density given by the leading term of eq. (14) with the product ($\kappa_0 d$).

We consider the coordinate z as the normal to the surface and the incidence plane is (y = 0), while the x axis represents the intersection of the incidence plane with the surface. By neglecting again any penetration inside the metal, the charge density of the *surface* plasmons is given by:

$$\rho_p(\boldsymbol{r},t) = \in_0 E_0 k \sin(2\theta_0) \times \frac{\left(1-\frac{\omega^2}{\omega_p{}^2}\right)\sin(\omega t - kx\sin\theta_0) - \omega\tau_0\cos(\omega t - kx\sin\theta_0)}{\left(1-\frac{\omega^2}{\omega_p{}^2}\right)^2 + \omega^2\tau_0{}^2} \approx \in_0 E_0 k \sin(2\theta_0)\frac{\sin(\omega t - kx\sin\theta_0)}{1-\frac{\omega^2}{\omega_p{}^2}} \quad (15)$$

where E_0 is the amplitude of the p wave and $k = 2\pi/\lambda$ the wavevector of the electromagnetic field, λ being its wavelength. It follows also that the most effective excitation of the surface plasmons occurs when $\theta_0 = 45°$.

One has to compare the amplitudes of the dipole induce charge modulations and of the plasmon amplitude:

$$\rho_{id}^{(\max)} \approx \frac{2.73P_0}{4\pi d^4}\left(1-\frac{\omega^2}{\omega_p{}^2}\right)^{-1} \text{ with}$$

$$\rho_p^{(\max)} \approx \in_0 E_0 k \sin(2\theta_0)\left(1-\frac{\omega^2}{\omega_p{}^2}\right)^{-1} \quad (16)$$

The factor 2.73 is just three times the value of the maximum of the function expressed in eq. (10):

$$h(u) = \frac{u\left(4-u^2\right)}{\left(u^2+1\right)^{7/2}} \quad (17)$$

By introducing again the polarizability and the polarization volume such that $P_0 = \alpha_0 E_0 = 4\pi\in_0 V_p$, and by considering $\theta_0 = 45°$, one obtains a simple condition for more intense amplitudes of plasmons when compared to that induced by the dipole:

$$\rho_{id}^{(\max)} < \rho_p^{(\max)} \quad \Rightarrow \quad d > (0.3V_p\lambda)^{1/4} \quad (18)$$

Several estimates may be done, but here let us just point that for V_p = 10 Å^3, the dipole induced charge amplitude variation is larger if the molecule is closer than about 1.2 nm to the substrate (λ = 700 nm). Note also that in the above considerations we introduced the 'standard' polarizability and polarization volume, in absence of the SERS effect, whereas one should take into account the SERS amplification factor. For instance, a polarization volume of 1 nm^3 (i.e. the polarizability of a simple molecule increased by two orders of magnitude, corresponding to a SERS amplification factor of 10^4-10^8) would induce prevalence of the dipole-induced charge variations for $d < 3.8$ nm.

Finally, one has to introduce the frequency dependent enhancement function $g(\omega)$:

$$g(\omega) = \frac{\left(1-\frac{\omega^2}{\omega_p{}^2}\right)}{\left(1-\frac{\omega^2}{\omega_p{}^2}\right)^2 + \omega^2\tau_0{}^2} \approx \frac{1}{1-\frac{\omega^2}{\omega_p{}^2}} \quad (\text{when } \omega\tau_0 << 1) \quad (19)$$

from the term with cos(ωt), eq. (13), into the derivation of the polarizability in presence of image dipoles. Thus, the equation for polarizability (5) has to be re-written as:

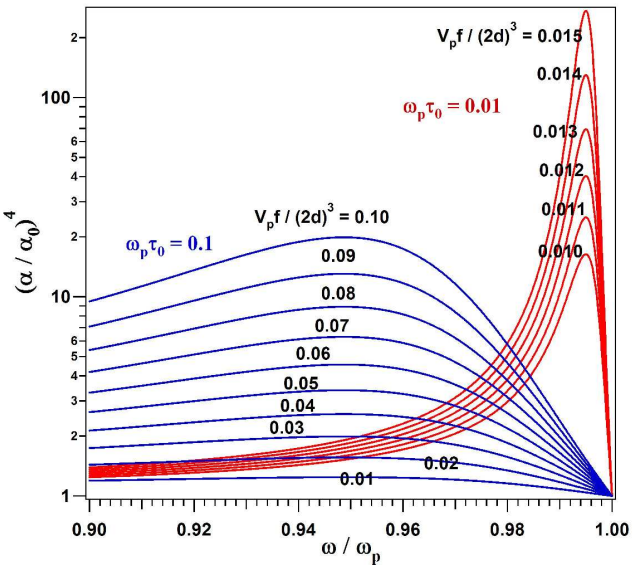

Fig. 7. The frequency dependence of the overall SERS enhancement factor, for two values of $V_pf/(2d)^3$ (red and blue series of curves) and for different values of the product $\omega_p\tau_0$. Please note the log scale.

$$\alpha = \frac{\alpha_0}{1-\frac{\alpha_0 f(d/R,\delta_0/R)}{4\pi\in_0(2d)^3}} = \frac{4\pi\in_0 V_p}{1-\frac{V_p f(d/R,\delta_0/R)}{(2d)^3}g(\omega)} \quad (20)$$

Thus, the denominator contains, in front of the ratio between the polarization volume and $(2d)^3$ the geometric enhancement factor discussed in the paragraph "Surface nanostructuring" together with a frequency enhancement factor $g(\omega)$. It is clear that the approximate formula for $g(\omega)$ explains immediately the strong enhancement factor when the light frequency approaches the plasma frequency in the metal. As stated above, from eq. (19) one can derive that the maximum of $g(\omega)$ occurs when $\omega = \omega_p + \Delta\omega = \omega_p(1 \pm \omega_p\tau_0)^{1/2} \approx \omega_p + 1/(2\tau_1)$, where we remind that τ_1 is the relaxation time in the metal. The maximum value of the frequency dependent enhancement function can be derived as being $g_{\max.} = 1/(2\omega_p\tau_0 - \omega_p{}^2\tau_0{}^2) \approx 1/(2\omega_p\tau_0) = (1/2) \times (\tau_1/\tau_0)^{1/2} = \omega_p/(4\Delta\omega)$.

Eq. (20) can be used to model the SERS enhancement factor, starting with basic knowledge of the vacuum polarizability of the molecule, geometric characteristics of the substrate, nature of the metal used (manifested by its plasmon frequency and conductivity). In fact, knowing the geometric enhancement factor f, the polarization volume of the molecule V_p and the distance of the molecule to the substrate d, one may determine the frequency where the maximum enhancement factor occurs, ω_m, by solving $g(\omega_m) = (2d)^3/(V_pf)$. Some frequency dependencies of the overall SERS enhancement factor α^4 are represented in Fig. 7. This picture analyzes unfavorable cases, where $\omega_p\tau_0 = (\tau_0/\tau_1)^{1/2}$ is rather large and the factor $V_pf/(2d)^3$ is away from unity. The frequency dependence is much sharper for low values of the product $\omega_p\tau_0 = (\tau_0/\tau_1)^{1/2}$. Therefore, good conductors are needed as SERS substrates and this supports also the prevalence of the effect on gold and silver substrates.

Also, in cases of larger distances from the molecule to the surface, the density amplitude from eq. (14) may be employed. But, as stated above, in such cases also plasmons become important and one has to introduce both charge densities from eqs. (15) and (14), then to retrieve numerically the electric field at the origin of the molecule. In this case, the simple approximation of interaction with the instantaneous image dipole formed in the metal will not be that accurate.

Examples of analyses

Frequency dependence of SERS signals

The distance of the molecules analyzed to the substrate may be estimated starting with eq. (20). Knowing the spectral dependence of the SERS amplification factor, one can infer the maximum of the frequency amplification function $g_{max.} \approx \omega_p/(2\Delta\omega)$. Thus, by introducing the geometric enhancement factor $f \approx \{2R/(2R - d)\}^3$, according to eq. (4) and the amplification factor of the polarizability $A = \alpha/\alpha_0$, the average distance of the molecules to the substrate may be derived as:

$$d = R\times\left\{1-\sqrt{1-\frac{1}{R}\left(\frac{V_p g_{max.} A}{A-1}\right)^{1/3}}\right\} \approx R\times\left\{1-\sqrt{1-\frac{1}{R}\left(V_p g_{max.}\right)^{1/3}}\right\} \quad (21)$$

where the approximation holds for large amplifications. Additionally, for large values of the typical radii R of the surface structures, the distance from the molecules to the substrate is given simply by:

$$d = \frac{1}{2}\left(\frac{V_p g_{max.} A}{A-1}\right)^{1/3} \approx \frac{\left(V_p g_{max.}\right)^{1/3}}{2} \quad (22)$$

as it might be derived also directly from eq. (2), introducing in addition the frequency dependent enhancement function. An application of the above formula starting with the values from Ref. [9] is presented in Table 1. The analyzed molecule is benzenethiol with vacuum polarizability of 11.93 Å^3 (Ref. [31]). Let us first remark that all data presented a blue shift of the maximum SERS amplification frequency with respect to the maximum of extinction, whereas from $g(\omega)$, eq. (19), when $\omega > \omega_p$ the function $g(\omega)$ becomes negative and the denominator of eq. (20) increases, therefore no enhancement factor should be observed ($\alpha < \alpha_0$). The key to solve this puzzle is to remark that the maximum of extinction corresponds to the surface plasmon resonance (SPR), ω_{sp}, of lower frequency than the bulk plasma frequency ω_p (in the ideal case of a flat interface between a perfect metal with air or vacuum $\omega_{sp} = \omega_p/2^{1/2}$). Indeed, for silver the plasmon frequency, as theoretically computed, is 9.2 eV, corresponding to ω_p = 13.96 PHz, whereas the measured value is 3.9 eV, corresponding to ω_p = 5.92 PHz[32]. From the shifts between the frequency of maximum amplification and the *bulk* or *surface* plasmon frequency (maximum of extinction) one derives $g_{max.}$ as:

$$g_{max.} = \frac{\omega_p^{\,4}}{\omega_p^{\,4} - \omega_m^{\,4}} = \frac{4\omega_{sp}^{\,4}}{4\omega_{sp}^{\,4} - \omega_m^{\,4}} \quad (23)$$

Then, eq. (22) is applied. The result for distances from molecules to the metal (Table 1) is in the range 1.2-1.3 Å, which implies that the Ag layer is quite few oxidized. For instance, standard photoelectron spectra of Ag foils *as introduced* yield the ration between the oxidized and the bulk metal around 0.1, therefore the oxide layer is at most 10 % of the inelastic mean free path[25] (around 12 Å[33]). XPS data obtained in our laboratory confirmed this ratio between the components corresponding to native Ag oxide layer and that of bulk Ag metal. Therefore, in average, the oxide layer has a thickness in the range of 1.1-1.2 Å, corresponding to less than one layer of Ag atoms undergoing oxidation at the surface.

Thus, the data from Ref. [9] may be analyzed by considering that the molecules are practically adsorbed on the AgFON SERS substrates and that quite few oxide layer is present on the surface, Consequently, the maximum SERS enhancement was obtained at rather low frequencies, as compared with the *bulk* plasma frequency. Incidentally, this frequency was close to the surface plasma frequency, but shifted towards higher frequencies. Now, if surface plasmons were the main responsible for the SERS effect in this case, it can be simply demonstrated that their frequency cannot exceed $\omega_{sp} = \omega_p/2^{1/2}$. Coupling to the surface nanostructures would eventually stabilize surface plasmons with lower values of the wavevector, therefore with even lower energies. Another effect to be taken into account would be a dielectric constant of the outer medium ($\in_r$) different from 1, which also lowers the surface plasmon frequency, in this case $\omega_{sp} = \omega_p/(1 + \in_r)^{1/2}$.

Table 1. Analysis of SERS data of benzenethiol for different substrates[9], exhibiting different plasmon frequencies: λ_p, ω_p are plasmon wavelength and frequency, respectively; λ_m, ω_m are the wavelength and the frequency of maximum SERS enhancement; EF is the enhancement factor, A is the polarizability amplification factor; $g_{max.}$ the maximum of the frequency dependent amplification function; d is the estimated distance of molecules to the substrate.

λ_p(nm)	λ_m(nm)	EF	A=EF$^{1/4}$	ω_{sp}(PHz)	ω_p(PHz)	ω_m(PHz)	$g_{max.}$	d(Å)
489	480	5.5x10^5	27.3	3.86	5.45	3.93	26.7	1.284
663	625	1.2x10^7	58.9	2.84	4.02	3.02	8.2	1.304
699	671	1.4x10^7	61.2	2.70	3.81	2.81	12.0	1.290
810	765	9.4x10^8	175	2.33	3.29	2.46	8.5	1.298

Note that the analyzed data from Fig. 4, taken from the same References, implied the formation of a dead layer of about 1 nm. It may happen that when atomic layer deposition of Al_2O_3 on AgFON is started, a further oxidation of the silver occurs prior to the deposition of alumina, owing to the presence of reactants and to a larger substrate temperature. Indeed, atomic oxygen reacts with silver yielding a limiting thickness of the oxide layer of about 12 Å,[34] which is in line with the thickness of the 'dead layer' derived in Fig. 4.

Temperature dependence

Figure 8 presents data extracted from Ref. [35], representing SERS signals of ethylene deposited on atomically clean, stepped

Cu(977), as function on temperature. The reason for analyzing these data is to investigate the validity of Eq. (8), that there should be a strong increase of the SERS signal at low temperature. The spectrum obtained at 150 K was not considered in this plot, since it has a much higher intensity that spectra obtained at lower temperatures, 120 K and 100 K. It may happen that, when the temperature is increased, more vibrational modes are excited and this may yield to an increase of the signal. However, the vibrational level investigated (1285 cm^{-1}) correspond to an excitation energy of about 0.16 eV, considerably larger than the thermal energy corresponding to 150 K (13 meV). Another effect not taken into account is the eventual dependence of the plasmon frequency on the temperature, which may yield non-monotonous temperature dependence of the SERS signal[36]. Such problems need to be investigated in more details, but in the following just the data exhibiting monotonous dependence of the SERS signal with temperature will be analyzed. Fig. 8(a) presents the raw data, Fig. 8(b) represents the SERS signal as function on the inverse of the temperature. It may be easily seen that one cannot conclude from these data that $I_{SERS} \sim 1/T$. Fig. 8(c) presents a $\log_{10}(I_{SERS})$ *vs*. $\log_{10}(T)$ plot, and from this representation it follows that $I_{SERS} \sim 1/T^2$ with a good approximation. Fig. 8(d) presents a plot of $\log(I_{SERS})$ *vs*. $1/T$ and one can see that these data can also be fitted by a straight line. This implies the validity of a model similar to that described by eq. (7), in the approximation of strong binding of molecules to the metal substrate, and with no equilibrium concentration of the molecules in absence of the attraction to the metal substrate, i.e.

$$n = n_0 \exp\left(\frac{P^2}{8\pi \in_0 (2d)^3 k_B T}\right) \qquad (24)$$

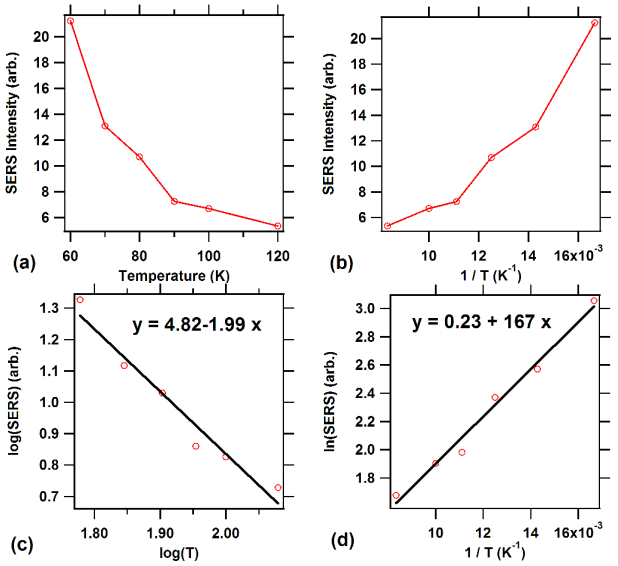

Fig. 8. Analysis of temperature dependencies of SERS signals of ethylene adsorbed on stepped Cu(977)[35]. (a) shows the extracted SERS signal as function on temperature, (b) represents a plot of the SERS signal as function on 1/T, (c) represents a log-log plot, together with a fit function, (d) represents the logarithm of the SERS signal as function on 1/T.

Just to estimate the orders of magnitude, we take into account the vacuum (α_0) molecular polarizability of ethylene[25], given by V_p = 4.252 Å^3, therefore the minimum distance from molecules to the substrate yields $d \approx 0.8$ Å. From the slope of the curve from Fig. 8(d) and introducing d (since molecules are deposited on atomically clean Cu), one obtains a dipole moment of about 1.45 x 10^{-30} C·m ≈ 0.43 D. The product between the amplitude of the exciting field and the enhancement factor yields as E x EF ~ $P/(4\pi\epsilon_0 V_p) \approx 3$ x 10^9 V/m, which is reasonable, for a typical electric field of 3 x 10^3 V/m, as estimated at the beginning of this paper, and an enhancement factor of 10^6. This example shows also how one can determine enhancement factors without having available Raman experiments performed on the same system, without the metal substrate.

Discussions and conclusions

Basic theoretical considerations discussed in this paper suggest that the SERS effect is favoured by any combination of the following situations:

(i) Small distances need to be achieved between the investigated molecules and the metal substrate, such that $2d$ approaches $V_p^{1/3}$. There is a strong dependence of the SERS signal on the distance d. Note that in Ref. [35] the Raman signal saturates for 1 L of ethylene adsorbed on Cu(110) at 45 K in ultrahigh vacuum (UHV).

(ii) Molecules should be placed into nanocavities (CERS), such that the geometric function $f(d/R, \delta_0/R)$ may increase by several units, going up to one order of magnitude increase. There is no need for these cavities to be disposed in regular arrays. *There is no need for expensive nanofabrication techniques*. Therefore, the SERS substrates need to be nanostructured, without well-defined ordered patterning, but with typical nanostructuring dimensions (e.g. radii of concavities) as close as possible to the typical dimensions of the molecules aimed to be investigated (on the order of $V_p^{1/3}$)[11]. Therefore, basic nanostructuring methods, such as the use of porous silicon[11] or the nanosphere litography[9,37] may be sufficient to provide low cost SERS substrates.

(iii) When the nanostructured surface presents concavities mimicking hemispheres, molecules placed in the centre of these hemispheres will be subject to a huge SERS enhancement factor.

(iv) The light frequency needs to approach the plasmon frequency of the metal; however, the SERS effect will be the most vigorous when the excitation frequency is a few tens or hundreds of cm^{-1} higher than the plasmon frequency, corresponding to a correction of $1/(2\tau_1)$ in ω. This effect is well demonstrated in Refs. [9,10], for example.

(v) Good conductors are needed as SERS substrates, because the frequency dependent function sharpen for low values of τ_0, i.e. for larger static conductivities.

(vi) Owing to the adsorption/desorption dynamics in a nonsolid medium (liquid or gas), the SERS effect is proportional to $\alpha^4 E^4$, therefore an increase of the polarizability by a factor or 10-20 suffices to explain the observed SERS enhancement factors. At high temperatures or low polarizabilities, when no significant agglomeration of molecules is found near the substrates owing to their interaction with image dipoles, the SERS effect remains proportional to E^2. Recent work proved experimentally the high dependence of the SERS on the way molecules and colloids are diluted and mixed together, yielding the fact that inhomogeneities in the distribution of colloids carrying molecules may be crucial for the signal obtained[38].

(vii) The substrates must be chemically inert for both keeping the metallic surface close to the adsorbed molecules and for avoiding too strong interactions with the analyzed molecules, resulting in conformational changes or charge transfer[35].

(viii) There should be a noticeable temperature effect, if one takes into account eq. (8). Actually, the temperature intervenes in the dynamics of adsorption-desorption on the metal surface. Note also that most of the data presented in Ref. [35] were obtained at low temperatures. Also, in Ref. [39] a clear enhancement of SERS signals at low temperatures was demonstrated from room temperature to 8.5 K, though not varying as $1/T$. After eight years of development, a setup named Cryo In-SEM offered a stronger increase in the SERS features when the samples are cooled[40]. It seems that this cryogenic area of Raman spectroscopy will have a considerable development in the near future. More theoretical work is needed to include other temperature effects, such as the population of the vibrational levels or the dependence on temperature of the plasmon frequency.

(ix) The SERS amplification factor is specific to the kind of molecules analyzed, since the 'polarization volumes" enter in a critical way at the denominator of any formula describing the effect - static, eq. (5), or dynamic, eq. (20). If the surface plasmons were the main responsible of the SERS effect, similar amplification factors would have been reported for quite different molecules. The literature is still elusive regarding this aspect. The actual considerations suggest a rather affirmative answer to the title of Chap. 5 of Ref. [28]: 'Is SERS molecule dependent?'

It was shown also that both field penetration effects into the metal and plasmons affect the very simple model proposed in this work, for distance ranges starting with 4 nm for simple molecules. Nevertheless, using image dipoles in case of small separation distance could simplify considerably the evaluations of SERS data and may lead to more quantitative evaluations, once e.g. the distance to the substrate, the nanostructuring and the molecular polarizabilities are accurately determined by other methods.

The actual results present also a possible drawback of SERS experiments: working on *too clean* substrates (molecules *too close* to the metal, small d), or on *too nanostructured* ones (large f), with *too large* polarizabilities (V_p), or *too close* to the plasma frequency (large g) may yield a too large factor $V_p f g/(2d)^3$, exceeding unity, therefore the molecule either will dissociate, or it will exhibit a permanent dipole moment (the case of a saturating function of the dipole moment on the applied field), eventually with low polarizability, since in that case $\partial P/\partial E$ is expected to decrease. It seems that choosing the right conditions for a good SERS experiment is rather delicate. The best is to have the ability to vary the excitation frequency, since the other factors are dictated by the molecules analyzed and by the substrate.

Experimental verifications of the assumptions from the present work may be undertaken by combining standard surface science UHV techniques with Raman spectroscopy, as for example in Ref. [35]. Such SERS experiments must be combined with other techniques able to probe the geometry of the molecules and their adsorption site in a non-invasive way, e.g. by photoelectron diffraction[41] or surface extended X-ray absorption fine structure[42], in order to assess precisely the molecule-substrate distance and the adsorption geometry. The SERS substrate need to be well characterized by scanning probe microscopic (SPM) techniques before starting the experiments. Last but not least, detailed SERS investigations as function on the temperature are needed, by further adaptation of the setups presented in Refs. [39,40] with other surface science analysis methods, possibly also using synchrotron radiation. I am confident that such data will be available soon, in order to check the very basic assumptions from this elemental theory and to render the SERS method more quantitative.

Finally, the actual considerations with image dipoles seems to be applicable also to surface enhanced infrared absorption (SEIRA). In this case, the excitation frequency is far away from the (surface of bulk) plasmon frequency of the metal, therefore $g \approx 1$ and rather a static model outlined in the first sections of this paper apply. It is clear that in absence of the frequency dependent amplification factor, low values in the denominator of eq. (20) will be more difficult to be achieved. For instance, in the case from Ref. [9] analyzed in Table 1, replacing $g_{max.} = 1$ in order to analyze the hypothetical case of low frequencies (SEIRA) yields $fV_p/(2d)^3 \approx 0.68$, therefore the polarizability increases by a factor or 3.1, and the enhancement factor would increase by at most a factor of 94. SERS remains therefore in some cases a more sensitive method than SEIRA, especially for small molecules, when the frequency dependent enhancement factor is needed to lower the denominator of eq. (20).

Nomenclature:

A = amplification of the polarizability = α/α_0 (dimensionless)
α = molecular polarizability (F x m^2)
α_0 = molecular polarizability in vacuum (F x m^2)
b = small value to be added to $(V_p f)^{1/3}$ in eq. (8) to yield $2d_{min.}$ (dimensionless)
β = second coefficient in the $P(E)$ series development = $(\partial^2 P/\partial E^2)_0$ (F x m^3/V)
dz = differential of z (m)
d = distance from a molecule to the metal substrate (m)
$d_{min.}$ = minimum distance of molecules to the substrate (m)
d_0 = 'dead layer', additional oxidized layer present of the Ag metal prior to the growth of Al_2O_3 (m)
δ_0 = separation distance between charges in a dipole (m)
Δd = uncertainity in the position of a molecule with respect to the metal surface (m)
$\Delta n(z)$ = deviation of the density of molecules from equilibrium owing to their attraction by the metal (m^{-3})
ΔS = analyzed area in the experiment (m^2)
$\Delta\omega$ = deviation of the frequency for maximum enhancement from the bulk plasmon frequency = $\omega_p - \omega_m$ (s^{-1})
e = elementary charge (1.602 x 10^{-19} C)
E = electric field, in general (V/m)
E_0 = amplitude of the oscillating electric field (V/m)
E_i = electric field of the image dipole inside a metal cavity (V/m)
$E_i^{(0)}$ = electric field of the image dipole near a metal plane (V/m)
$E_{ext.}$ = external electric field (V/m)
$E_{ind.}$ = induced electric field by the image dipole (V/m)
EF = SERS enhancement factor (dimensionless)
$\in_0$ = permittivity of vacuum (8.854 x 10^{-12} F/m)
$\in_r$ = relative permittivity of a material (dielectric constant) (dimensionless)
$\varepsilon_0(z)$ = binding energy to a metal plane = $- U_a(z)$ (J)

f = nanostructuring (geometric) factor, see eq. (4) (dimensionless)
F_a = force of attraction from the metal surface (N)
$g(\omega)$ = frequency dependent enhancement function, introduced in eq. (13) (dimensionless)
$g_{max.}$ = maximum of the function $g(\omega)$ (dimensionless)
$h(u)$ = function used to abbreviate eq. (10), mainly to derive its maximum value (dimensionless)
i = imaginary unit, $i^2 = -1$ (dimensionless)
I_{SERS} = empirical SERS intensity (arb. units)
j = current density (A/m^2)
k = wavevector for electromagnetic wave or of surface plasmon propagation (m^{-1})
k_B = Boltzmann constant (1.381×10^{-23} J/K)
κ_0 = inverse of the skin depth (see the ESI) (m^{-1})
λ = wavelength of electromagnetic radiation (m)
m = molecular mass (kg)
m^* = effective mass of electrons in the metal (kg)
n = electron density in a metal (m^{-3})
n_0 = density of molecules at equilibrium (m^{-3})
ν = frequency of exciting electromagnetic wave = $\omega/(2\pi)$ (s^{-1})
P = dipole moment, in general (C x m)
P_p = permanent molecular dipole moment (C x m)
q = value of (±) charges separated into a dipole ($P = q \times \delta_0$) (C)
θ_0 = incidence angle of the electromagnetic wave on the surface, exciting surface plasmons (radians)
$\boldsymbol{r}$ = vector coordinate, most often in the ($z = 0$) plane (m)
R = radius of a cavity (or of a nanoparticle) (m)
ρ_{ids} = static density of charge induced in a metal plane by a dipole placed above the surface (m^{-3})
ρ_{id} = dynamic density of charge induced in a metal plane by an oscillating dipole placed above the surface (m^{-3})
$\rho_0(\boldsymbol{r})$ = amplitude of ρ_{id}, such that $\rho_{id}(\boldsymbol{r}, t) = \rho_0(\boldsymbol{r})\exp(i\omega t)$ (m)
$\tilde{\rho}$ = density, when penetrating effects of the field into the metal are taken into account (see the ESI) (m^{-3})
$\rho_{id}^{(max.)}$= maximum of ρ_{id} (m^{-3})
$\rho_p(\boldsymbol{r}, t)$ = charge density associated to the plasmons (m^{-3})
$\rho_p^{(max.)}$= maximum of ρ_p (m^{-3})
$\sigma(\omega)$ = frequency-dependent (Drude) conductivity ((Ω x m)$^{-1}$)
σ_0 = static conductivity ((Ω x m)$^{-1}$)
t = time (s)
T = temperature (K)
τ_1 = relaxation time with respect to collisions with impurities in a metal (Boltzmann equation) (s)
$\tau(\varepsilon_F)$ = value of the relaxation time at the Fermi energy (s)
τ_0 = characteristic electron relaxation time = σ_0/ϵ_0 (s)
u = variable in the function $h(u)$ (dimensionless)
$U_a(z)$ = attraction potential energy towards the metal surface (J)
V_p = polarization volume of a molecule = $\alpha/(4\pi\epsilon_0)$ (m^3)
$\langle v \rangle$ = average molecular speed, Maxwell-Boltzmann statistics (m/s)
x, y = coordinates parallel to the metal plane (m)
z = coordinate normal to the plane of the substrate (m)
ξ = dimensionless parameter = $2d_{min.}/(V_p f)^{1/3}$
ω = frequency of exciting radiation = $2\pi\nu$ (s^{-1})
ω_p = bulk plasmon frequency = $(ne^2/(\epsilon_0 m^*))^{1/2}$ (s^{-1})
ω_{sp} = surface plasmon frequency = $\omega_p/2^{1/2}$ (s^{-1})
ω_m = frequency for the maximum of $g(\omega)$ (s^{-1})

Acknowledgements

This work was supported by the UEFISCDI - PN II - PCA No. 128/2011 and by PN09-450101/2009 Contracts granted by the Romanian Ministry of Education.

Notes and references

[a] *National Institute of Materials Physics, Atomistilor 105b, 077125 Măgurele-Ilfov, Romania. Fax: 40 21369 0177; Tel: 40 72429 1045; E-mail: teodorescu@infim.ro*

† Electronic Supplementary Information (ESI) available: [details of any supplementary information available should be included here]. See DOI: 10.1039/b000000x/

1. K. Kneipp, M. Moskovits and M. Kneipp, (Eds.) *Surface-Enhanced Raman Scattering. Physics and Applications*, *Top. Appl. Phys.* 2003, **103**, Springer, Berlin.
2. M. Fleischmann, P.J. Hendra and A.J. McQuillan, *Chem. Phys. Lett.*, 1974, **26,** 163–166.
3. M.G. Albrecht and J.A. Creighton, *J. Am. Chem. Soc.*, 1977, **99,** 5215–5217.
4. D.L. Jeanmaire and R.P. Van Duyne, *J. Electroanal. Chem.*, 1977, **84,** 1–20.
5. K. Kneipp, Y. Wang, H. Kneipp, L.T. Perelman, I. Itzkan, R.R. Dasari, and Michael S. Feld, *Phys. Rev. Lett.*, 1997, **78,** 1667-1670.
6. S.L. Kleinman, E. Ringe, N. Valley, K.L. Wustholz, E. Phillips, K.A. Scheidt, G.C. Schatz, and R.P. Van Duyne, *J. Am. Chem. Soc.*, 2011, **133,** 4115-4122.
7. J.M. Pitarke, V.M. Silkin, E.V. Chulkov, and P.M. Echenique, *Rep. Prog. Phys.*, 2007, **70,** 1-87.
8. E.D. Diebold, N.H. Mack, S.K. Doom, and E. Mazur, *Langmuir*, 2009, **25,** 1790-1794.
9. J.A. Dieringer, A.D. McFarland, N.C. Shah, D.A. Stuart, A.V. Whitney, C.R. Yonzon, M.A. Young, X. Zhang, and R.P. Van Duyne, *Faraday Discuss.*, 2006, **132**, 9–26.
10. P.L. Stiles, J.A. Dieringer, N.C. Shah, and R.P. Van Duyne, *Annu. Rev. Anal. Chem.*, 2008, **1,** 601–626.
11. T. Ignat, R. Munoz, K. Irina, I. Obieta, M. Miu, M. Simion, and M. Iovu, *Superlattices Microstr.*, 2009, **46,** 451-460.
12. K.C. Vernon, T.J. Davis, F.H. Scholes, D.E. Gómez, and D. Lau, *J. Raman Spectrosc.*, 2010, **41,** 1106-1111.
13. M.G. Weber, J.P. Litz, D.J. Masiello, and K.A. Willets, *ACS Nano*, 2012, **6,** 1839-1848.
14. P. Alonso-González, P. Albella, M. Schnell, J. Chen, F. Huth, A. García-Etxarri, F. Casanova, F. Golmar, L. Arzubiaga, L.E. Hueso, J. Aizpurua and R., *Nat. Commun.*, 2012, **3**, 684.
15. T. Coenen, E.J.R. Vesseur and A. Polman, *ACS Nano*, 2012, **6,** 1742–1750.
16. B.T. Draine and P. Flatau, *J. Opt. Soc. Am. A*, 1994, **11,** 1491-1499.
17. W. Luo, W. van der Veer, P. Chu, D.L. Mills, R.M. Penner, and J.C. Hemminger, *J. Phys. Chem. C*, 2008, **112**, 11609-11613.
18. T. Ignat, M.-A. Husanu, R. Munoz, M. Kusko, M. Danila, and C.M. Teodorescu, *Thin Solid Films*, 2014, **550**, 354-360.
19. H.A. Kramers and W. Heisenberg, *Z. Phys.*, 1925, **31**, 681–708.
20. D.R. Lide (Ed.-in-Chief), *CRC Handbook of Chemistry and Physics, 75th Ed.*, 1994, CRC Press, Boca Raton, p. **10**-192.
21. J.D. Jackson, *Classical Electrodynamics, 3rd Ed.*, 1999, Wiley, Hoboken, Chapter 2.
22. G. Grosso and G. Pastori Parravicini, *Solid State Physics*, 2003, Academic Press, San Diego, p. 340.
23. K. Tkacz-Smiech, A. Kolezynski and W.S. Ptak, *Ferroelectrics*, 2000, **237**, 57-64.
24. K.W. Kolasinski, *Surface science: foundations of catalysis and nanoscience, 3rd Ed.*, 2012, Wiley, Hoboken, Chapter 3.
25. B.V. Crist, *Handbooks of Monochromatic XPS Spectra, Vol. 1: The Elements and Native Oxides*, 2004, XPS International LLC, Mountain View, p. 315.
26. B. Pettinger, B. Ren, G. Picardi, R. Schuster, and G. Ertl, *Phys. Rev. Lett.*, 2004, **92,** 096101.

27. D.-K. Lim, K.-S. Jeon, J.-H. Hwang, H. Kim, S.H. Kwon, Y.D. Suh, and Jwa-Min Nam, *Nat. Nanotech.*, 2011, **6,** 452-460.
28. R. Aroca, *Surface-Enhanced Vibrational Spectroscopy*, 2006, Wiley, Chichester.
29. J.P. Srivastava, *Elements of Solid State Physics*, Third Edition, 2011, PHI Learning, New Delhi, p. 338.
30. N.W. Ashcroft and N.D. Mermin, *Solid State Physics*, 1976, Saunders College, Philadelphia, p. 16. See also http://en.wikipedia.org/wiki/Drude_model
31. http://www.hmdb.ca/metabolites/HMDB33746 accessed on 14/12/05.
32. C. Noguez, *J. Phys. Chem. C*, 2007, **111**, 3806-3819
33. S. Hüfner, *Photoelectron Spectroscopy: Principles and Applications*, 3rd Edition, 2003, Springer, Berlin, p. 9.
34. A. de Rooij, *ESA J.*, 1989, **13**, 363-382.
35. C. Siemes, A. Bruckbauer, A. Goussev, A. Otto, M. Sinther, and A. Pucci, *J. Raman Spectrosc.*, 2001, **32,** 231–239.
36. H.P. Chiang, P.T. Leung and W.S. Tse, *J. Phys. Chem. B*, 2000, **104**, 2348-2350.
37. B. Sharma, M. Fernanda Cardinal, S.L. Kleinman, N.G. Greeneltch, R.R. Frontiera, M.G. Blaber, G.C. Schatz, and R.P. Van Duyne, *MRS Bull.*, 2013, **38**, 615-624.
38. B.L. Darby and E.C. Le Ru, *J. Am. Chem. Soc.*, 2014, **136**, 10965−10973.
39. P. Anger, A. Feltz, T. Berghaus, A.J. Meixner, *J. Microsc.-Oxford* , 2003, **209**, 162-166.
40. J. Hazekamp, M.G. Reed, C.V. Howard, A.A. Van Apeldoorn, and C. Otto, *J. Microsc.-Oxford*, 2011, **244**, 122-128.
41. D.P. Woodruff, and A.M. Bradshaw, *Rep. Prog. Phys.*, 1994, **57,** 1029-1080.
42. J. Stöhr, in *X-Ray Absorption: Principles, Applications, Techniques of EXAFS, SEXAFS and XANES*, D. Koningsberger and R. Prins, (Eds.) 1988, Wiley, Hoboken, p. 443.